Heterogeneous Integration of Spin-photon Interfaces with a Scalable CMOS Platform

Li, Linsen; De Santis, Lorenzo; Harris, Isaac; Chen, Kevin C.; Christen, Ian; Trusheim, Matthew; Han, Ruonan; Englund, Dirk

DOI
10.1364/CLEO_FS.2024.FW3K.2

Publication date
2024

Document Version
Final published version

Published in
CLEO 2024: Conference on Lasers and Electro-Optics

Heterogeneous Integration of Spin-photon Interfaces with a Scalable CMOS Platform

Linsen Li,[1,2,*] Lorenzo De Santis,[1,3], Isaac Harris,[1,2] Kevin C. Chen,[1,2] Ian Christen,[1,2] Matthew Trusheim,[1,2] Ruonan Han,[1,2] and Dirk Englund[1,2,*]

[1] *Research Laboratory of Electronics, Massachusetts Institute of Technology, Cambridge, MA 02139*
[2] *Electrical Engineering and Computer Science, Massachusetts Institute of Technology, Cambridge, MA 02139*
[3] *QuTech, Delft University of Technology, PO Box 5046, 2600 GA Delft, Netherlands.*

[*] *linsenli@mit.edu, englund@mit.edu*

Abstract: We introduce a quantum system-on-chip (QSoC) architecture based on (I) a co-designed diamond quantum memory array, (II) a custom CMOS backplane, and (III) a protocol for fully connected cluster state generation. © 2024 The Author(s)

1. Introduction

Diamond color centers have emerged as the leading solid-state platform for quantum technologies and have recently achieved a quantum advantage in secret key distribution [1]. Recent theoretical works [2] estimate that general-purpose quantum computing using local quantum communication networks will require thousands of logical qubits encoded from millions of physical qubits, which presents a substantial challenge to the hardware architecture at this scale. To address the unanswered scaling problem, we introduce a modular hardware architecture "Quantum System on Chip" (QSoC) that features compact two-dimensional arrays "quantum microchiplets" (QMCs) containing tin-vacancy (SnV^-) spin qubits integrated on custom CMOS backplane [3]. We demonstrate crucial architectural features with a high-throughput calibration of the QSoC for spin-qubit spectral inhomogenous registration and spin-qubit spectral tuning functionality for inhomogenous compensation.

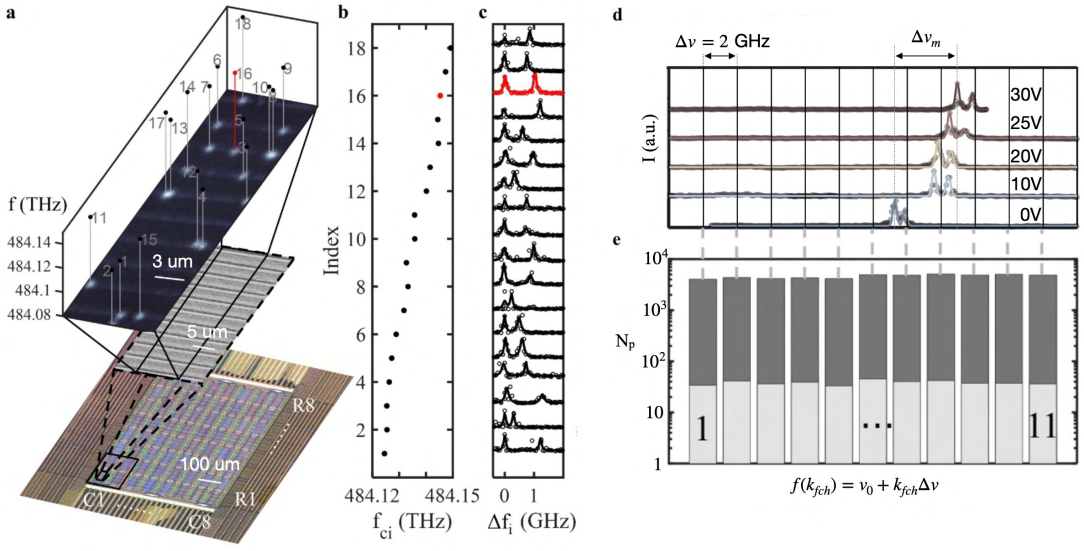

Fig. 1. **a,** An overlay of the optical microscope, SEM, and superposition EMCCD image of emitters' bright frames. **b,** The ZPL frequency f_{ci} of the emitter with index *i* in **a**. **c,** The PLE spectrum of the emitters in **a** with f_{ci} frequency shifted. **d,** Voltage-induced tuning for an emitter crossing various frequency channels. **e,** The emitter bright spots number statistics for 11 frequency channels.

2. Inhomogeneous registration and tuning

The QSoC is fabricated by large-scale lock-and-release hybrid integration of diamond QMC (fabricated by the undercut process) and post-processed CMOS backplane control chip [3]. We perform a high-throughput characterization of QSoC using optical excitation with wide-field illumination and readout from an electron-multiplying

charge-coupled device (EMCCD) [4]. Figure 1 shows the inhomogeneous quantum emitter registration with wide-field characterization. We show an example of this measurement on a QMC in Fig. 1. Figure 1a presents the spatial locations of SnV^- in the central QMC region. Figure 1b shows the ZPL frequency of the color centers f_{ci}, and their normalized photoluminescence excitation (PLE) spectra are reported in Figure 1c.

Figure 1d illustrates the tuning of an emitter from frequency channel $k_{fch} = 7$ to $k_{fch} = 8$ at varying voltages. The spectral tuning range from the minimum tuning voltage to the maximum tuning voltage, defined as $\Delta\nu_m$, is shown in the figure. The histograms in Fig. 1e represent the number of emitters found in each frequency channel with light gray for a single field of view (FOV) and dark gray for all 1024 quantum channels of the entire QSoC.

3. Further scaling and discussion

Figure 2a illustrates how a connected qubit graph can be built using experimental single FOV data at 11 frequency channels. In a single FOV, the emitters have all-to-all connectivity within frequency channels with optical routing, and some of the emitters can be tuned across neighbor frequency channels. Figure 2b presents the quantum circuit of equivalence with the cluster in Fig. 2a, assuming each frequency channel k_{fch} has $m_{k_{fch}}$ emitters. A desired quantum algorithm can be compiled for the connectivity of the system. The red line labeled here corresponds to the red line in Fig. 2a. Figure 2c indicates the ratio of the fully connected qubit graph to the total number of qubit nodes (p_c) as a function of the average frequency tunability ratio ($\overline{\Delta\nu_m}/\nu_{inh}$) across the entire inhomogeneous range (ν_{inh}) under different sizes of the qubit system (N_{qubit}). This plot shows that for larger system scales, a lower tunability requirement for achieving a fully connected qubit graph allows the system to operate with lower tuning voltages for better energy efficiency. Figure 2d illustrates the scaling potential of the QSoC platform, considering the number of qubits (N_{qubit}) and the number of direct connections per qubit (N_{link}). The light gray box, which includes the smaller scattered points, represents the data from a single FOV, while the dark gray box, including the larger scattered points, represents the data from the entire sample area. Two gray boxes include the results of a single frequency channel ($k_{max} = 1$) and 11 frequency channels ($k_{max} = 11$).

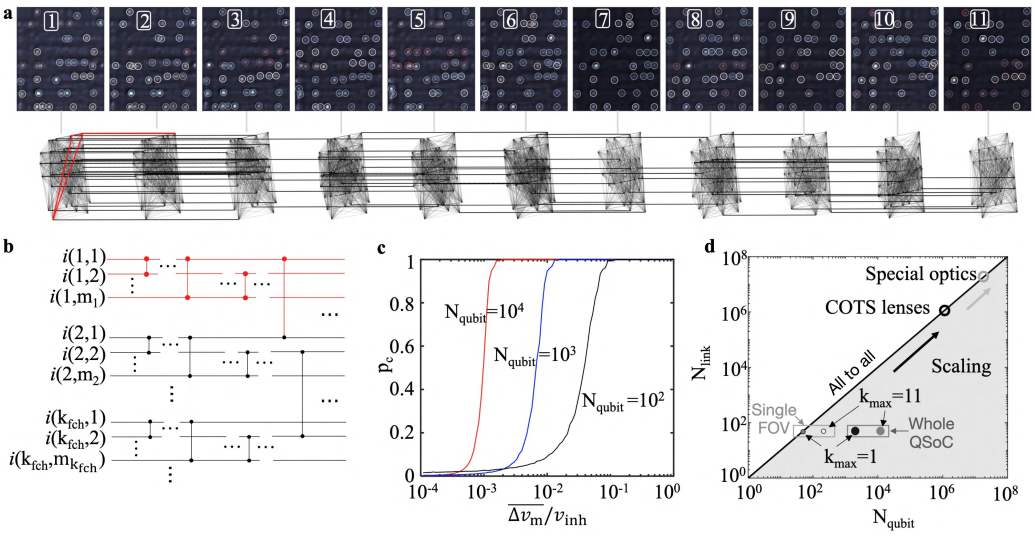

Fig. 2. **a,** Widefield images across 11 frequency channels (k_{fch} from 1 to 11) and the illustration of connected cluster using the widefield data from a single field of view. **b,** The quantum circuit representations of the connected qubit graph. **c,** The ratio of the fully connected qubit graph p_c against $\overline{\Delta\nu_m}/\nu_{inh}$ under various N_{qubit}. **d,** The scaling potential of the QSoC platform considering N_{qubit} and N_{link}. The shading indicates the potential scaling of the system with the all-to-all connectivity.

References

1. M.K. Bhaskar et al., Experimental demonstration of memory- enhanced quantum communication. Nature 580 (7801), 60–64. (2020)
2. H. Choi et al., Percolation-based architecture for cluster state creation using photon-mediated entanglement between atomic memories. npj Quantum Information 5(1), 1–7. (2019)
3. L. Li et al., Heterogeneous integration of spin-photon interfaces with a scalable CMOS platform. ArXiv:2308.14289. (2023)
4. M. Sutula et al., Large-scale optical characterization of solid-state quantum emitters. Nature Materials pp. 1–7. (2023)